JOURNAL OF Materials CHEMISTRY

Extended X-ray absorption fine structure study of manganese–oxo species and related compounds on the surface of MCM-41 channels

Robert Burch, Neil A. Cruise, David Gleeson and Shik Chi Tsang

The Catalysis Research Centre, Department of Chemistry, University of Reading, UK RG6 6AD

It has been previously shown that passing $Mn_2(CO)_{10}$ vapour over MCM-41 mesoporous silica at 50 °C followed by heat treatment in air resulted in a material with high catalytic activity for propene oxidation. EXAFS studies of the $Mn_2(CO)_{10}$ precursor, MCM-41 treated with $Mn_2(CO)_{10}$ before and after the calcination in air have therefore been carried out and the results are presented in this paper. Upon immobilisation of the $Mn_2(CO)_{10}$, the EXAFS data indicate four Mn—(CO) groups with a Mn—Mn interaction at 3.112 Å; new interactions such as Mn—O (at the much shorter distance of 1.705 Å) and Mn—Si (*via* Mn—O—Si) at a distance of 3.529 Å are evident. This clearly suggests that the Mn species anchor onto the surface of MCM-41 forming Mn—O—Si bonds, presumably through the reaction of surface silanol and Mn carbonyl species. After heat treatment in air, the EXAFS data indicate further loss of carbonyl groups with the formation of more Mn—O interactions (three Mn—O at 1.900 Å and one Mn—O at 1.747 Å). The best fitted model for the surface Mn–oxo species has a structure resembling Mn_2O_7. With reference to this structure, an active site in the Mn–modified MCM-41 for propene oxidation is therefore proposed.

The recent synthesis of mesoporous silica materials by the co-operative assembly of silica and surfactants has attracted a great deal of research interest.[1] The mesoporous silicate shows regular arrays of uniform channels and the pore diameter can be varied by using surfactants of different alkyl chain lengths. Mesoporous silicas are generally characterised by having larger pores and larger internal surface areas ($>1\,000\ m^2\ g^{-1}$) than those of known molecular sieves. Thus, these materials have the potential to be used as size and shape selective catalysts for bulky reactants, such as may be of interest to the fine chemical and pharmaceutical industries. However, silica displays a low catalytic activity for many reactions. Attempts to synthesise other active mesoporous oxides or the incorporation of small amounts of transition metals into the framework of the mesosilicates during their synthesis have therefore been reported. Success is limited to elements such as Al, Ti, V, Nb, Ta and Hf in which the mesoporous phase can still be maintained.[2–5]

It is known that MCM-41 silica contains many surface silanol groups, so an alternative strategy is to use the mesoporous silica as a template for the deposition of reactive linings of chemical species through the surface reaction of Si—OH groups on the walls of the MCM-41 channels with various organometallic species. A wide variety of surface-anchored species on the surface of MCM-41 can be made successfully by this method. Some of the MCM-41 supported species have been claimed to display a high catalytic activity.[6–8] On the other hand, there is very limited work in elucidating the structures of these MCM-41 supported species, particularly in an attempt to correlate the structures with their catalytic activities.

Recently, we reported a novel MCM-41 based Mn-containing catalyst which was obtained by reacting gaseous $Mn_2(CO)_{10}$ with MCM-41 silica by the chemical vapour deposition (CVD) technique at 50 °C, followed by calcination in air.[9] Transmission electron microscopy and EDX analysis showed that the Mn species were very evenly distributed on the surface of the materials. Atomic absorption analysis showed a high loading of 8.5% m/m of Mn on the MCM-41. This catalyst exhibited high activities for the oxidation of CO and propene, and this was attributed to the high reactivity of the Mn–oxygen species. In this paper we show that extended X-ray absorption fine structure (EXAFS) analysis of the Mn–modified MCM-41 can provide structural information about the surface-attached Mn—O species. From the proposed structural model, an active site for CO and propene oxidation is proposed.

Experimental

Preparation of Mn–oxo species on the surface of MCM-41

All manipulations were carried out under an inert atmosphere or under vacuum. $Mn_2(CO)_{10}$ was purchased from Aldrich and used without further purification. The MCM-41 (pore diameter 30 Å) was prepared according to a previously described method.[1] The MCM-41 was then degassed under a stream of flowing nitrogen for 2 h at 300 °C. The MCM-41 (100 mg) and $Mn_2(CO)_{10}$ (50 mg) were placed in an open-ended tubular silica vessel and a quartz-wool plug was used to separate the two materials. The reactor was inserted into a box furnace. The reactor was then pumped and flushed with nitrogen three times, after which the vacuum was left on. The furnace was heated to 50 °C. Periodically nitrogen was allowed to flow through the reactor for the even distribution of the manganese species on the MCM material. Finally, the treated material was heated in air for 2 h at 300 °C to give an intense brown coloured material.[9]

EXAFS experiment

EXAFS data were collected for the following three materials: sample **A**, $Mn_2(CO)_{10}$; sample **B**, MCM-41 treated with $Mn_2(CO)_{10}$; sample **C**, sample **B** heated in air at 300 °C. The preparation procedures were as follows: sample **A**, $Mn_2(CO)_{10}$ (purity 98%) was obtained from Aldrich Chemical Co. and used without further purification; sample **B**, 50 mg $Mn_2(CO)_{10}$ (excess) was sublimed through 100 mg degassed MCM-41 at 50 °C under a dynamic vacuum (10^{-4} Torr); sample **C**, after the sublimation of $Mn_2(CO)_{10}$ through MCM-41, the mixture was then calcined at 300 °C for 2 h as previously reported.[9]

Manganese K-edge X-ray absorption spectra were recorded over 13.5 $Å^{-1}$ K range on Station 7.1 at the Synchrotron Radiation Source (SRS) at the Daresbury Laboratory, UK, operating in transmission mode at 2 GeV and 125 mA. The Si(111) monochromator was adjusted to give 70% harmonic rejection. Samples were finely ground and diluted with BN. Approximately 2 mm thickness of the powder was held in an

aluminium holder between sheets of Sellotape. Two scans were recorded for each sample at 77 K.

A general expression[10] used in the interpretation of EXAFS data, which relates structural parameters to measured EXAFS oscillations, is:

$$\chi(k) = -A(k)\Sigma_j(N_j/kR_j^2)|f_j(k,\pi)|\exp(-2\sigma_j^2k^2) \times \exp(-2R_j/\lambda)\sin(2kR_j+2\delta_1+\psi_j)$$

where $\chi(k)$ is the magnitude of EXAFS as a function of the photoelectron wavevector k; N_j is the number of identical scattering atoms at an average interatomic distance R_j in the jth co-ordination shell; the terms $2\delta_1+\psi_j$ are phase shifts experienced by the photoelectron during the outgoing and scattering process, and $f_j(k, \pi)$ is the backscatter amplitude of the photoelectron wave; λ is the mean free path of the photoelectron. There is also a Debye–Waller factor which depends on σ_j^2, the mean variation in R_j. The elastic mean free path λ and $A(k)$, an amplitude factor, measure the proportion of absorption events that result in excitation of a single photoelectron. The EXAFS data were normalised, averaged and analysed using EXCALIB, EXBACK and EXCURV92.[11] The phase shift terms in the above equation are obtained within EXCURV92 using *ab initio* calculations. Fitting the experimental spectrum in k space involves calculating a spectrum using an assumed set of parameters R, N, A until a best least-squares fit is obtained. Multiple scattering methods were employed for M—C—O shells.[12] Crystallographic data and absorption spectra for comparable. Mn compounds are used as appropriate (see later). Statistical errors are given in parentheses when a best least-squares fit is obtained for the refined parameters.

Results

Table 1 shows the result of the curve fitting analysis of EXAFS data collected for sample **A** [$Mn_2(CO)_{10}$], which gave five Mn—C distances at 1.85 Å and five Mn—O distances at 3.023 Å. The bond distances of Mn—C and Mn—O (*via* Mn—C—O) are in good agreement with the published crystal structure,[13] which is also consistent with the literature values for other metal carbonyls (Cr—C 1.89 Å, Cr—C—O 3.01 Å; Fe—C 1.796 Å, Fe—C—O 2.917 Å) studied by the EXAFS technique.[14] The $Mn_2(CO)_{10}$ structure is shown in Scheme 1(*a*). Since the difference between the axial and equatorial distances is very small, we found no distinction between axial or equatorial CO groups in the EXAFS data. Fig. 1 shows a Mn—Mn distance of 3.11 Å which is best fitted to the curve. The value is slightly longer than 2.90 Å obtained from the single crystal X-ray diffraction data.[13]

Fig. 2 and Table 2 show the EXAFS analysis of sample **B** [surface immobilised $Mn_2(CO)_{10}$ on MCM-41]. Four Mn—C distances at 1.876 Å, four Mn—O distances at 3.013 Å and a Mn—Mn distance at 3.112 Å could be derived. New interactions such as a Mn—Si distance at 3.529 Å and a shorter Mn—O distance of 1.705 Å were apparent from the analysis.

Table 1 Structural data for $Mn_2(CO)_{10}$

coordination number	atom type	EXAFS distance/Å	Debye–Waller factor	X-ray crystal structure bond distance/Å[13]
5	C	1.850(3)	0.008(6)	4 × 1.85 (equatorial) 1 × 1.81 (axial)
5	O	3.023(3)	0.005(7)	4 × 2.99 (equatorial) 1 × 2.95 (axial)
1	Mn	3.111(7)	0.002(11)	2.90

ef = −4.28(25), R = 24.18, FI = 0.00039, Mn—C—O 177(5)° (177.03[10]).

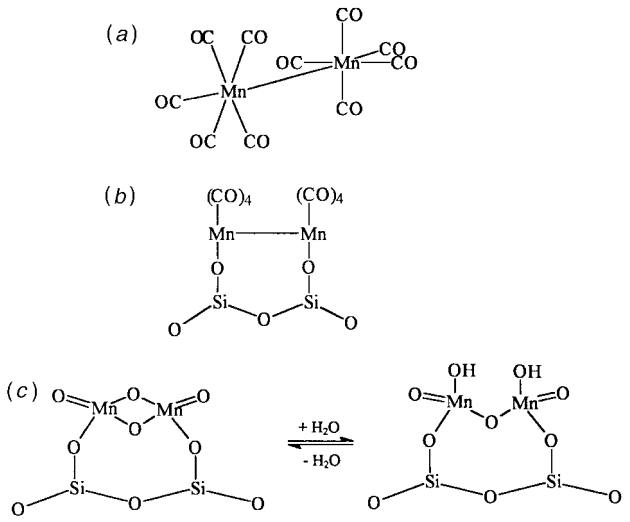

Scheme 1 Proposed structures of the Mn species. (*a*) Sample **A**, $Mn_2(CO)_{10}$ precursor; (*b*) sample **B**, surface immobilised $Mn_2(CO)_{10}$ on the surface of MCM-41 channels before calcination; (*c*) sample **C**, two closely related Mn-oxo species grafted onto the walls of MCM-41.

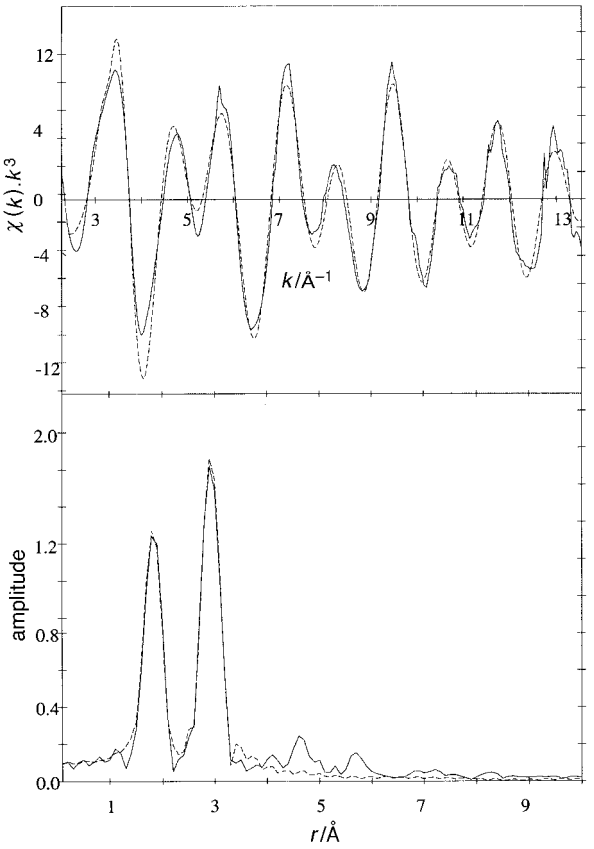

Fig. 1 Mn K-edge EXAFS spectra for $Mn_2(CO)_{10}$ (sample **A**), recorded at 77 K

In addition, our previous IR studies of surface immobilised $Mn_2(CO)_{10}$ on MCM-41 showed the presence of CO bands [of different chemical environment to $Mn_2(CO)_{10}$ species] prior to calcination.[9] We therefore postulate that $Mn_2(CO)_{10}$ loses two CO groups upon immobilisation to the internal walls of the MCM-41 *via* two Si—O—Mn bonds.

Studies of $Mo(CO)_6$ interactions with silica gel, MCM-41 silica, MgO, ZrO_2, TiO_2, and γ-alumina have been reported.[15] It was shown that $Mo(CO)_6$ is molecularly bound to the MCM-41 silica at room temperature and all the carbonyl ligands are liberated to CO in a single step upon heating to *ca.* 171 °C. In contrast, other metal oxide surfaces induce an

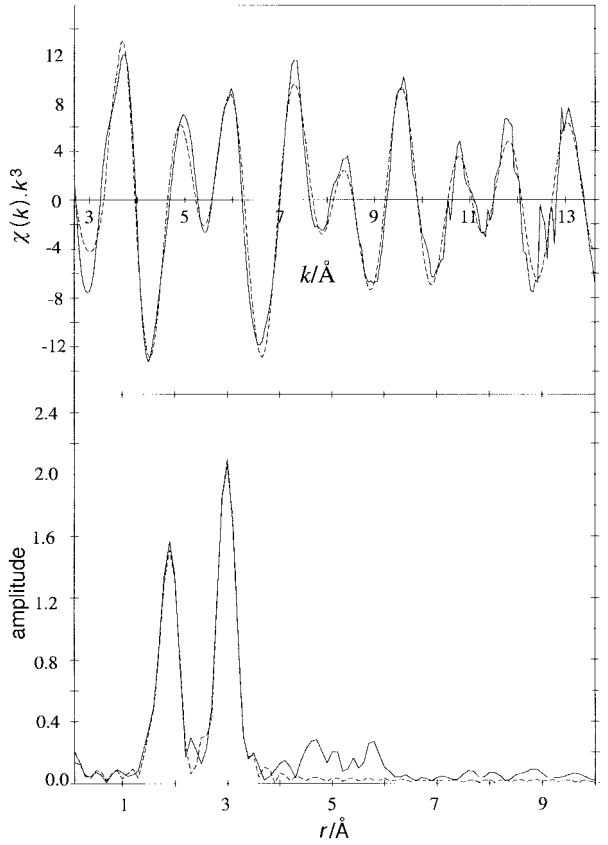

Fig. 2 Mn K-edge EXAFS spectra for the surface immobilised $Mn_2(CO)_{10}$ species on the surface of the MCM-41 channels before calcination in air (sample **B**), recorded at 77 K

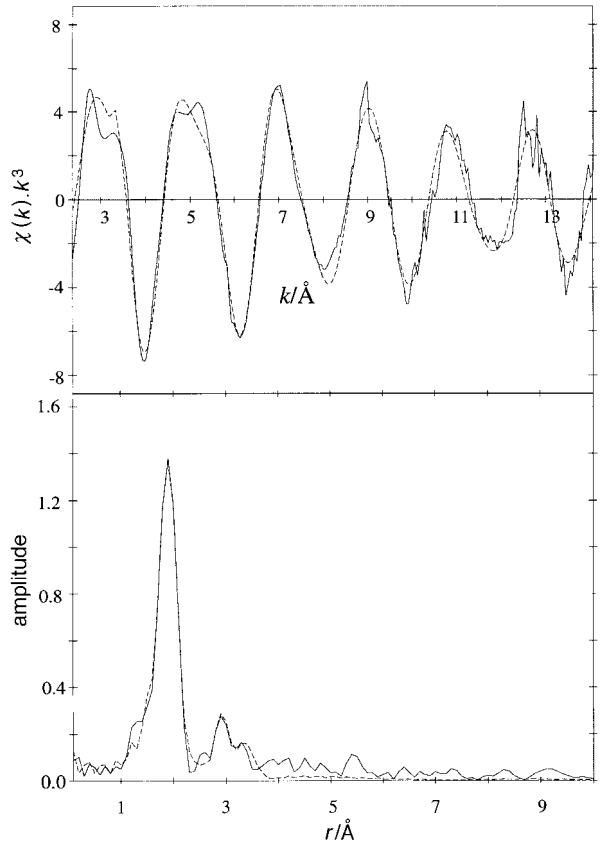

Fig. 3 Mn K-edge EXAFS spectra for the Mn modified MCM-41 after air calcination (sample **C**), recorded at 77 K

Table 2 Structural data for surface immobilised $Mn_2(CO)_{10}$ on MCM-41

coordination number	atom type	EXAFS distance/Å	Debye–Waller factor
1	O	1.705(9)	0.010(7)
4	C	1.876(3)	0.013(3)
4	O	3.013(4)	0.005(2)
1	Mn	3.112(14)	0.002(1)
1	Si	3.529(18)	0.004(2)

ef = −1.90(25), R = 27.14, FI = 0.00055.

initial loss of three CO ligands forming quasi-stable $[Mo(CO)_3]_{ads}$ species before further decomposition. This has been assigned to the nucleophilic substitution of the CO group by the free electron pairs of the surface O^{2-} or OH groups, the strength of which depends on the metal cations.

From the above work, it is conceivable that Mn is directly bound to the surface of MCM-41 through the nucleophilic substitution reaction of Si—OH groups with the carbonyl species. The Mn—Si interaction at 3.529 Å is due to the Mn—O—Si distance. The Mn—O distance at 1.705 Å could be attributable to a Mn—O—Si distance or to a Mn=O distance. Attempts to fit an O shell at a longer Mn—O—Si distance resulted in a bond distance at 2.12 Å. This had a very large negative Debye–Waller factor and, according to the Joyner *et al.* significance test,[11] this shell was not significant at the 5% level and gave only a negligible reduction in the fit index. The Mn—O distance at 1.705 Å was significant according to the Joyner *et al.* significance test[11] and significantly improved the fit index. The overview of the surface-anchored Mn species before heat treatment is in Scheme 1(*b*).

We emphasise that sample **B** was made by passing an excess of $Mn_2(CO)_{10}$ through the MCM-41 materials at 50 °C, which resulted in a very high Mn loading (8–10% m/m Mn). Thus, we cannot discount the fact that some unbound $Mn_2(CO)_{10}$ and reaction intermediates may be entrapped inside the mesoporous silica. EXAFS data will average out the interactions should there be a mixture of related species. Thus, the model in Scheme 1(*b*) should not be taken literally. However, the formation of a Mn—O—Si linkage undoubtedly suggests that the Mn carbonyl species is chemically immobilised on the surface of the MCM-41.

The best EXAFS fitted data of the sample **C** are given in Table 3. The overall fits for all the elements and their corresponding distances were obtained, in some cases employing the third and fourth shells. Adding more of these cells considerably improved the fit of the EXAFS data.

Despite the extensive data fitting, the analyses show no Mn—C interaction. This clearly suggests that all the residual carbonyls were either decomposed or detached from the Mn atom during the heat treatment. The best fitted model also suggests three Mn—O distances at 1.900 Å and one Mn—O distance at 1.747 Å. The shorter distance at 1.747 Å could be attributed to a Mn=O double bond. The three Mn—O distances of the same value could be the result of averaging three Mn—O single bonds in different chemical environments giving an overall distance of 1.900 Å. The Mn—Si interaction with distance of 3.280 Å is due to the Mn—O—Si moiety. We

Table 3 Structural data for Mn-modified MCM-41

coordination number	atom type	EXAFS distance/Å	Debye–Waller factor
1	O	1.747(7)	0.005(2)
3	O	1.900(2)	0.002(1)
1	Mn	2.931(9)	0.016(2)
1	Si	3.280(17)	0.012(4)

ef = −5.79(33), R = 27.36, FI = 0.00051.

Table 4 Mn—O and Mn—Mn distances in structurally comparable compounds

compound	bond	bond distance/Å	ref.
MnO_2	Mn—O	1.88	18
	Mn—Mn	2.87	
Mn_2O_3	Mn—O	1.99	19
Mn_2O_7	Mn—O_{term}	1.59	20
	Mn—O_{br}	1.77	
Mn_5O_8	Mn—O	1.88	21
	Mn—Mn	2.86	
$K_6Mn_2O_6$	Mn—O_{term}	1.86	16
	Mn—O_{br}	1.94	
Li_2MnO_3	Mn—O_{br}	1.91	22
	Mn—Mn	2.87	
$Na_2Mn_3O_7$	Mn—O_{br}	1.90	23
	Mn—Mn	2.79–2.96	
{[(bispicMe$_2$en)Mn]$_2$(μ-O)(μ-OAc)}(ClO$_4$)$_3$	Mn—O_{oxo}	1.79	24

br = bridging; term = terminal; bispicMe$_2$en = *N*,*N*′-bis(2-pyridylmethyl)-*N*,*N*′-dimethylethane-1,2-diamine.

propose at least one of the two remaining single Mn—O bonds is a bridging oxygen formed between the neighbouring Mn species. This is supported by the data fit which was improved when a Mn—Mn distance of 2.931 Å was added. The heat treatment in air could generate the bridging oxygen between the two separate but nearby Mn species (sample B), which clips the two Mn atoms together.

If the two bridging oxygens exist between two Mn atoms, this surface anchored molecule is structurally similar to the $[Mn_2O_6]^{6-}$ [16] unit of edge-sharing tetrahedra (oxygen atoms occupy the corner positions). It is also possible that one of the single Mn—O bonds comprises Mn—OH resulting from hydrolysis in moist air. Thus, the two tetrahedra would be joined, in this case, by corner-sharing oxygen. This structure resembles closely the structure of Mn_2O_7 which can be obtained by the dehydration of two manganoic acid units ($HMnO_4$, which can be made by treating potassium permanganate with strong acid). Preliminary experiments suggest an acidic nature for sample **C**.

It is noted that both of the two possible structures which are given in Scheme 1(*c*) can account for the EXAFS data. Unfortunately, EXAFS offers no detection of hydrogen atoms and the difference in the bond distances is too small for their differentiation. Ideally, IR spectroscopy might be able to differentiate the two structures since the MnO_3—O— moiety in Mo_2O_7 or related structures displays characteristic absorption bands near 800–1000 cm^{-1}.[17] Unfortunately, we found that MCM-41 silica gave a very strong and broad absorption band in the same region masking any diagnostic peaks which might be present.[1] Table 4 summarises structural information on typical examples of Mn–oxygen species for comparison with our data.

Active site for propene and CO oxidation

We have reported that Mn–modified MCM-41 shows high activity for the oxidation of propene[9] and CO[25] compared with supported and unsupported solid state Mn oxides. The EXAFS analysis clearly suggests that the surface-anchored Mn species on MCM-41 are structurally very similar to molecular Mn–oxo entities such as MnO_4^-, Mn_2O_7 or $Mn_2O_6^{6-}$ displaying discrete tetrahedra. It is therefore conceivable that the propene molecule is attached to the Mn by oxidative addition followed by subsequent oxygen attack. This is a typical oxidation mechanism commonly displayed in molecular Mn–oxo catalysts.

A catalyst having a discrete molecular nature is in marked contrast to the three-dimensional repetitive units observed in many manganese oxide lattices where most of the Mn–oxygen ions are buried deep inside the bulk. In many cases, the oxidation rates over the solid materials are limited by the mass transfer of the reactive species. Thus high reaction temperatures are necessary. For comparison, a discrete molecule of Mn_2O_7 is a very powerful oxidising agent which can cause explosion in contact with many reducing reagents even above 50 °C. It is believed that our MCM-41 supported Mn species structurally resembles Mn_2O_7. However, because of the anchoring bonds (*via* Mn—O—Si) the Mn is in a lower oxidation state (v). The combination of high surface exposure and the molecular nature of anchored Mn species on the MCM-41 makes the resulting solid material a rather special and unique oxidation catalyst. In particular, the discrete but chemically immobilised molecular catalyst is expected to be more thermally stable at elevated temperatures and to be more readily regenerated by an oxidation treatment in air. The use of such a material as a regenerable, stoichiometric, oxidation reagent is one possible application of this novel material.

Conclusions

These results demonstrate that EXAFS can be used to provide structural information on the nature of the Mn catalyst species on the internal surfaces of the MCM-41 channels, which would otherwise not be obtainable by other means. We have followed the change in the Mn environment from the $Mn_2(CO)_{10}$ precursor to the surface immobilisation of species on the MCM-41 before and after heat treatment in air. Immobilisation of gaseous $Mn_2(CO)_{10}$ within the channels results in fragmentation of the parent dimer leading to $Mn(CO)_4$ moieties anchored through the Mn—O—Si bonds. The Mn–oxo species grafted onto the internal walls of MCM-41 after heat treatment in air appears to be dimeric in form, and connected by the bridging oxygen atom(s). The active site for propene oxidation is thought to be related to the high oxidation state Mn with its terminal Mn=O bond. These structural models are derived from the best fitted EXAFS data with no implications for any dynamic structures during catalytic reactions.

We thank the EPSRC for support (GR/K60381), Dr F. W. C. Mossellmans, Dr S. Hibble and Dr F. Bradey for helpful discussions, and the Daresbury Laboratory for use of the SRS and other facilities.

References

1 C. T. Kresge, M. E. Leonowicz, W. J. Roth, J. C. Vartuli and J. S. Beck, *Nature (London)*, 1992, **359**, 710.
2 P. T. Tanev, M. Chibwe and T. J. Pinnavaia, *Nature* (*London*), 1994, **368**, 321.
3 D. M. Antonelli, A. Nakahira and J. Y. Ying, *Inorg. Chem.*, 1996, **35**, 3126.
4 D. M. Antonelli and J. Y. Ying, *Chem. Mater.*, 1996, **8**, 874.
5 P. Liu, J. Liu and A. Sayari, *Chem. Commun.*, 1997, 577.
6 T. Maschmeyer, F. Rey, G. Sankar and J. M. Thomas, *Nature* (*London*), 1995, 159.
7 R. Ryoo, C. H. Ko, J. M. Kim and R. Howe, *Catal. Lett.*, 1996, **37**, 29.
8 C. P. Mehnert and J. Y. Ying, *Abstr. Pap. Am. Chem. Soc.*, 1997, 213, Pt. 1, 312-COLL.
9 R. Burch, N. A. Cruise, D. Gleeson and S. C. Tsang, *Chem. Commun.*, 1996, 951.
10 S. J. Gurman, *J. Synchrotron Radiat.*, 1995, **2** , 56.
11 N. Binsted, J. W. Campbell, S. J. Gurman and P. C. Stephenson, EXCURV92, Daresbury Laboratory, Warrington, 1992; U. Von Barth and L. Hedin, *J. Phys. C.*, 1972, **5**, 1629; L. Hedin and S. Lundqvist, *Solid State Phys.*, 1969, **23**, 1; R. W. Joyner, K. J. Martin and P. Meehan, *J. Phys. C.*, 1987, **20**, 4005.
12 N. Binsted, S. C. Cook, J. Evans, G. N. Greaves and R. J. Price, *J. Am. Chem. Soc.*, 1987, **109**, 3669; N. Binsted, J. Evans, G. N. Greaves and R. J. Price, *J. Chem. Soc., Chem. Commun.*, 1987, 1330.
13 M. R. Churchill, K. N. Amoh and H. J. Wasserman, *Inorg. Chem.*, 1981, **20**, 1609.

14 I. Beattie, P. J. Jones and N. A. Young, *J. Am. Chem. Soc*., 1994, **114**, 6149
15 H. G. Ang, K. S. Chan, G. K. Chuah, S. Jaenicke and S. K. Neo, *J. Chem. Soc., Dalton Trans*., 1995, 3753.
16 R. Hoppe, *Angew. Chem., Int. Ed. Engl*., 1981, 2063.
17 W. Levason, J. S. Ogden and J. W. Turff, *J. Chem. Soc., Dalton Trans*., 1983, 2699.
18 W. H. Baur, *Acta Crystallogr., Sect. B*, 1976, **32**, 220.
19 R. Norrestam, *Acta Chem. Scand*., 1967, **21**, 2871.
20 R. Dronskowski, *Z. Anorg. Allg. Chem*., 1988, **7**, 558.
21 H. R. Oswald and M. J. Wampetich, *Helv. Chim. Acta*, 1967, **50**, 2023.
22 P. Strobel and B. Lambert-Andron, *J. Solid State Chem*., 1988, **75**, 90.
23 F. M. Chang and M. Jansen, *Z. Anorg. Allg. Chem*., 1985, **531**, 177.
24 N. Arulsamy, J. Glerup, A. Hazell, D. J. Hodgson, C. J. McKenzie and H. Toftlund, *Inorg. Chem*., 1994, **33**, 3023.
25 R. Burch, N. A Cruise, D. Gleeson and S. C. Tsang, unpublished results.

Paper 7/03739B*; Received* 29*th May*, 1997